Effects of Uniaxial Stress on Excitons in CuCl

T. Koda, T. Murahashi, and T. Mitani
Department of Applied Physics, University of Tokyo, Bunkyo-ku, Tokyo, 113 Japan

and

S. Sakoda and Y. Onodera
Department of Physics, University of Kyoto, Sakyo-ku, Kyoto, 606 Japan
(Received 21 June 1971)

The effects of uniaxial stress on the exciton reflection spectra of zinc-blende CuCl have been investigated experimentally and theoretically. From a comparison of the experimental results with a theory which takes account of the strain, spin-exchange, and stress-induced k-linear terms, it is established that the stress-induced k-linear term is playing an essential role in the anomalous transverse-longitudinal mode mixing of the Z_3 exciton observed in a configuration of $\vec{P} \parallel [001]$ and $\vec{K} \parallel [110]$. The coefficient of the stress-induced k-linear term is estimated to be about 10^{-7} eV cm, which seems to be reasonable in comparison with the previously known k-linear term in CdS. It is further proved that this effect is closely related to a stress-induced gyrotropy in deformed CuCl from macroscopic considerations on the dielectric tensor with a spatial dispersion linear in $\vec{K}$. Additional contribution of the effect of an off-axis incidence in case of lower symmetry is also discussed.

I. INTRODUCTION

The effects of uniaxial stress on excitons have been attracting a considerable interest in this decade. In an early stage of the study, the stress-induced changes in the exciton spectra were simply related to deformation-induced changes in the relevant one-electron energy bands. Here the exciton wave functions were assumed to be simple products of the hole (or missing electron) and electron wave functions associated with particular valence and conduction bands. A number of works have been reported using this approximation method, mostly concerned with experimental determinations of the deformation-potential constants of the relevant energy bands.[1]

It has recently been gradually recognized, however, that the spin-exchange interaction in an electron-hole pair produces a considerable change in the exciton spectra by a configuration mixing of exciton levels in the j-j coupling scheme, as has been first pointed out by Onodera and Toyozawa.[2] The exchange, when combined with a strain, gives rise to a splitting of exciton levels which is unexpected in the simple deformation-potential treatment. Observation of the stress-exchange splitting of excitons in wurtzite II-VI crystals demonstrated this effect most conspicuously.[3] Several studies have subsequently been reported on the stress-exchange coupling effects on excitons in II-VI crystals[4] and GaAs.[5]

Recently it has been proved further that the uniaxial stress effect reveals more profound aspects of excitons in quite a prominent way, namely, we have observed an unusual reflection anomaly in the uniaxially deformed CuCl which cannot be accounted for by the existing theory.[6] Subsequently, this phenomenon has been investigated theoretically by two of the authors and successfully accounted for by the introduction of the stress-induced k-linear terms in the usual exciton matrix formalism.[7] In this way we are formulating a more and more refined theory for the uniaxial stress effects on excitons.

However we would like to point out here that the importance of the uniaxial stress effects on excitons does not merely lie in a sophistication of theory, but in their relationship to more general aspects of crystal optics in which excitons play a dominant role. In an artificially deformed crystal under an external stress, we can realize various circumstances treated in crystal optics such as the usual ($\vec{K}$-vector-independent) optical birefringence and an optical anisotropy linear in $\vec{K}$ (gyrotropy). As shown in the present paper, we can investigate these macroscopic optical properties in terms of a microscopic view of excitons.

This paper deals with a detailed account of the experimental and theoretical investigation of the effects of uniaxial stress on excitons in CuCl. Although the study is not complete enough in a quantitative sense, because of various problems involved in a quantitative analysis of the experimental results, it is believed to be worthwhile to report our present understandings on the phenomenon we have investigated for uniaxially deformed CuCl. Emphasis will be placed mainly on a semiquantitative description of the basic features of the phenomenon and on general aspects of excitons in crystal optics.

A theoretical framework of exciton states in deformed CuCl is presented in Sec. II. In Sec. III, a detailed account of the experimental results is

given, followed by a semiquantitative comparison with the theoretical results. Section IV is devoted to a phenomenological interpretation of the results in terms of the stress-induced gyrotropy as well as to discussions pertaining to the stress-induced k-linear effect. Section V is a summary and contains our concluding remarks on the subject. In the Appendix, microtheoretical support is given to the phenomenological considerations on the dielectric-constant tensor developed in Sec. IV A.

II. THEORY OF EXCITONS IN UNIAXIALLY DEFORMED CuCl

A. Brief Survey on Exciton States in CuCl

Basic features of the energy-band structure of zinc-blende CuCl are established by several previous studies.[8] The Γ_1 conduction band (Γ_6 in double-group notation) is s-like, while the Γ_5 valence band is composed of Cu $3d$ orbitals hybridized with Cl $3p$ orbitals. The negative spin-orbit splitting in the Γ_7 (upper) and Γ_8 (lower) valence bands is ascribed to a larger amount of the Cu $3d$ component.[9] Both of the conduction and valence bands have extrema at the Γ point as is the case in most of zinc-blende semiconductors. The electron and hole effective masses are not accurately determined yet, but the hole mass is supposed to be considerably large because of the d-orbital-rich valence band.

Two direct exciton states associated with the Γ_7 and Γ_8 valence bands are called the Z_3 and $Z_{1,2}$ excitons, respectively, by Cardona.[10] Since the spin-orbit splitting of the hole, $\lambda = -63$ meV, is considerably larger than the electron-hole spin-exchange energy $\Delta_T = 8.7$ meV,[11] the resulting exciton levels follow approximately a j-j coupling scheme. The exciton wave functions, the Γ_5 and Γ_2 excitons for the Z_3 band and the Γ_5, Γ_3, and Γ_4 excitons for the $Z_{1,2}$ band, have been derived in Ref. 7 as the proper linear combinations of the missing valence-electron–conduction-electron pairs.

B. Energy Band under Stress

In order to formulate an effective-mass equation for excitons under uniaxial stress, which will be given in Sec. II C, it is necessary to investigate the energy spectra of the relevant one-electron energy bands under stress. The valence-band energy spectrum can be derived from the Γ_5 (T_2) bases at $\vec{k}=0$ by introducing the spin-orbit, strain, and $\vec{k}\cdot\vec{p}$ energies as perturbations. Within the first-order approximation of these perturbations, the spin-orbit interaction is responsible for the spin-orbit splitting of the Γ_5 band into the Γ_7 and Γ_8 bands, while the strain yields the usual deformation-potential terms. The third perturbation, the $\vec{k}\cdot\vec{p}$ term, vanishes in first order because of the time-reversal symmetry in the zinc-blende CuCl.[12]

When we proceed to the second-order effects, this $\vec{k}\cdot\vec{p}$ term gives rise to the usual kinetic energy of the valence electron which is quadratic in $\vec{k}$. In addition, we have to include a term which is bilinear in $\vec{k}\cdot\vec{p}$ and strain in the same order of approximation.[13] Usually such a term is quite small in magnitude, but nevertheless an effect arising from this term turns out later to play an essential role in the presently observed exciton spectra under uniaxial stress.

The explicit form of the valence-band energy spectrum $E_v(\vec{k}, e_{ij})$ in the presence of the strain tensor e_{ij} is expressed in terms of $\{\mu\} = \{b_x\alpha, \ldots, b_z\beta\}$ as follows:

$$E_v(\vec{k}, e_{ij}) = [E_k(\vec{k}) + E_D(e_{ij}) + E_{kD}(\vec{k}, e_{ij})]\hat{1} - (\tfrac{1}{3}\lambda)\vec{l}\cdot\vec{\sigma}\,, \tag{1}$$

with

$$E_k(\vec{k}) = A_0 k^2\hat{1} + A_1[(l_x^2 - \tfrac{1}{3}l^2)k_x^2 + \text{c.p.}] + A_2[(l_x l_y + l_y l_x)k_x k_y + \text{c.p.}]\,, \tag{2}$$

$$E_D(e_{ij}) = D_0^v(e_{xx}+e_{yy}+e_{zz})\hat{1} + D_1[(l_x^2 - \tfrac{1}{3}l^2)e_{xy} + \text{c.p.}] + D_2[(l_x l_y + l_y l_x)e_{xy} + \text{c.p.}]\,, \tag{3}$$

and

$$E_{kD}(\vec{k}, e_{ij}) = [B(e_{xy}k_y - e_{zx}k_z) + C(e_{yy} - e_{zz})k_x]l_x + \text{c.p.} \tag{4}$$

Here the b_i's are three Bloch states belonging to the Γ_5 valence band; $\vec{l}$ ($|\vec{l}| = 1$) is an angular momentum operator with the components l_x, l_y, and l_z; and σ is the Pauli spin matrix. c.p. denotes cyclic permutations with respect to the indices, x, y, and z. In this expression, $E_k(\vec{k})$ corresponds to the kinetic energy of the valence electron, $E_D(e_{ij})$ to the usual strain Hamiltonian, and $E_{kD}(\vec{k}, e_{ij})$ to the stress-induced k-linear terms, which are bilinear in strain and $\vec{k}\cdot\vec{p}$ term. The appearance of the last energy term is permissible in the absence of the inversion symmetry in the zinc-blende structure.

There can also exist, in principle, other k-linear terms. They are the first-order term derived from a perturbation of $(\hbar/2mc)^2(\vec{\sigma}\times\vec{\nabla}V)\cdot\vec{k}$ and a second-order term bilinear in $\vec{k}\cdot\vec{p}$ and spin-orbit interaction. However, it can be shown that these intrinsic k-linear terms existing in an unstrained CuCl are sufficiently small to be safely neglected in the present consideration.[7]

As for the Γ_6 conduction band, the energy $E_c(\vec{k}, e_{ij})$ is expressed in terms of $\{\nu\} = \{s\alpha, s\beta\}$ simply by

$$E_c(\vec{k}, e_{ij}) = A_0^c k^2\hat{1} + D_0^c(e_{xx}+e_{yy}+e_{zz})\hat{1}\,. \tag{5}$$

Here s is the Bloch function of the Γ_1 conduction band.

Consequently, the whole energy spectrum of the conduction and valence bands in strained CuCl is expressed by a set of parameters; A_0^c, A_0, A_1, and A_2 for the electron and hole masses, respectively, the deformation-potential constants D_0^c, D_0^v, D_1, and D_2, and the coefficients of the stress-induced k-linear term B and C. Experimental estimation of some of these parameters is attempted in Sec. III C from a study of the uniaxial stress effects on exciton spectra.

C. Exciton Matrix under Stress

Exciton states in deformed CuCl are derived from the one-electron energy spectrum under stress described in Sec. II B. The effective-mass equation for excitons with wave vector $\vec{K}$ formed by these energy bands is given by

$$\sum_{\{\mu',\nu'\}} E_{\mu\nu;\mu'\nu'} F_{\mu'\nu'}(\vec{r}) = EF_{\mu\nu}(\vec{r}) , \tag{6}$$

where

$$E_{\mu\nu;\mu'\nu'} = \delta_{\mu\mu'} E^c_{\nu\nu'}(\tfrac{1}{2}\vec{K} - i\vec{\nabla}) - \delta_{\nu\nu'} E^v_{\mu'\mu}(-\tfrac{1}{2}\vec{K} - i\vec{\nabla})$$

$$+ \delta_{\mu\mu'}\delta_{\nu\nu'} V(\vec{r}) + \Omega J_{\mu\nu;\mu'\nu'}\delta(\vec{r}) . \tag{7}$$

The first two terms in (7) represent the kinetic energies of the electron and hole, respectively. The third term corresponds to the Coulombic attraction energy which is diagonal with respect to the different (μ,ν) pairs. The last term is the electron-hole exchange energy. Ω stands for the volume of the unit cell. $J_{\mu\nu;\mu'\nu'}$ consists of two different kinds of terms: One is the direct exchange interaction similar to that appearing in the atomic excitation, while the other corresponds to the long-range resonance interaction between the exciton dipole moments and is responsible for the longitudinal and transverse splitting of the exciton levels. We shall neglect the participation of energy bands other than the lowest Γ_6 conduction and the highest Γ_7 and Γ_8 valence bands, which is supposed to be reasonable in view of the band structure of CuCl. Then the exciton effective-mass equation (6) is constructed from the 12 electron-hole pair states (μ,ν). Here μ and ν refer, respectively, to the missing electron states in the valence bands and to the electron states in the conduction band.

This 12×12 effective-mass equation is solved by a perturbation method in the following way: First, the strain and exchange terms are momentarily ignored. Further, we neglect the off-diagonal elements of the kinetic energy of hole. The latter neglect is equivalent to assuming spherical energy bands for hole, which is justified on account of the heavy-hole mass in CuCl. Then the effective-mass equation reduces to a completely diagonal 12×12 matrix. Assuming a $1s$ hydrogenic function for the zeroth-order envelope function $F(r)$, the strain and exchange terms are calculated by the eigenstates of this diagonal matrix. The resulting 12×12 matrix which includes nondiagonal exchange and strain terms is finally diagonalized. The 12 eigenenergies and eigenvectors obtained by this procedure correspond to all the exciton states associated with the Z_3 and $Z_{1,2}$ bands under a particular stress.

The most important feature of this exciton matrix is that nonvanishing off-diagonal elements exist even within the submatrix for the (Γ_7, Γ_6) pair corresponding to the Z_3 exciton band before diagonalization. These off-diagonal elements originate from the stress-induced k-linear term $E_{kD}(-\frac{1}{2}\vec{K} - i\vec{\nabla}, e_{ij})$ and give rise to a stress-induced coupling between the different exciton states belonging to the Z_3 band. A similar situation is also found in the $Z_{1,2}$ band. Such a coupling depends on the direction of the applied uniaxial stress and will be described in more detail later for several configurations in comparison with the experimental results.

As a result of such diagonalization of the exciton matrix with strain, we can calculate the energy spectrum of the Z_3 and $Z_{1,2}$ exciton bands as a function of the strain, or, if we know the elastic constants of CuCl, of the applied uniaxial pressure $\vec{P}$ for a particular configuration of $\vec{P}$ and $\vec{K}$ with respect to the crystallographic axes. Such calculation can also predict the polarization characteristics and the relative intensities of the respective exciton states under stress. In order to get numerical results which can be compared with the experimental results, we have to determine of course the values of the parameters appearing in the exciton matrix. We choose the spin-orbit splitting $\lambda = -63$ meV, the transverse exchange energy $\Delta_T = 8.7$ meV, and the longitudinal exchange energy $\Delta_L = 24.9$ meV according to the magneto-optical results of Staude.[11] The elastic compliance constants at liquid-helium temperature are tentatively estimated from the room-temperature values reported by Inoguchi *et al.*[14] by reducing them by 10%, taking into account the increased stiffness at lower temperatures. The assumed elastic constants are $s_{11}^E = 7.5_1\times10^{-12}$, $s_{12}^E = -3.0_6\times10^{-12}$, and $s_{44}^E = 5.7_1\times10^{-12}$ cm^2/dyn. The remaining parameters are the deformation-potential constants and the coefficients of the stress-induced k-linear terms, which are to be estimated from the uniaxial stress measurements as described in Sec. III.

III. EXPERIMENTAL RESULTS AND COMPARISON WITH THEORY

A. Experimental Procedure

Samples were cut from ingots of single-crystal

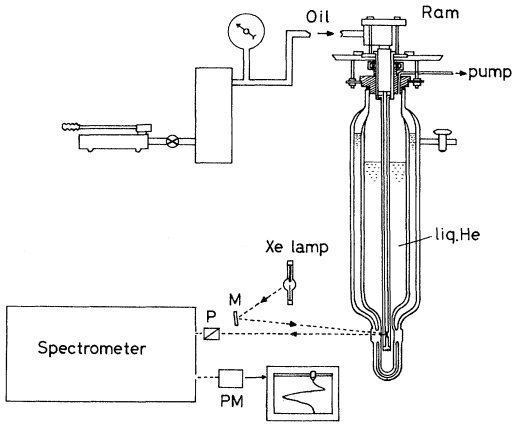

FIG. 1. Schematic diagram of the experimental system.

CuCl grown by the Bridgman method and were polished to the parallelepipeds of about $3\times3\times4$ mm in size. The sample surfaces were oriented by the x-ray Laue reflection measurements to the particular crystallographic planes within an accuracy of a few degrees. In total, 12 samples were used for the uniaxial stress measurements in the five different experimental configurations as described below. Several samples were subjected to a thermal annealing treatment (at 390 °C for 45 h and subsequent slow cooling) prior to the optical measurements, but since no significant difference was found in the optical spectra of annealed and unannealed samples, most of samples were used without annealing treatment.

After chemically etching with concentrated HCl solution, the sample was mounted in a glass liquid-helium Dewar vessel for the uniaxial stress measurements. The pressure apparatus used in this experiment is similar to that described in Ref. 4. The sample was immersed in liquid helium pumped below the λ point and the reflection spectra were measured photoelectrically in a nearly normal incidence condition (the deviation from it was less than 5°) by a Jarrell-Ash 3.4-m grating spectrograph with the inverse dispersion of 0.24 nm. The photon energies were calibrated by a superposition of the 388.865-nm line of He. The experimental assembly is schematically illustrated in Fig. 1.

B. Experimental Results

The experimental configurations employed in the present uniaxial measurements are specified by the direction of the applied uniaxial pressure $\vec{P}$ and the $\vec{K}$ vector of the incident light, respectively, with respect to the particular crystallographic axis, and by the polarization of the $\vec{E}$ vector of the light. Since the pressure was always perpendicular to $\vec{K}$ ($\vec{K}\perp\vec{P}$) in the present measurements, the spectra were measured for the $\vec{E}\parallel\vec{P}$ and $\vec{E}\perp\vec{P}$ polarizations. The measurements were made on the following five experimental configurations: $\vec{P}\parallel[001]$, $\vec{K}\parallel[110]$; $\vec{P}\parallel[001]$, $\vec{K}\parallel[100]$; $\vec{P}\parallel[111]$, $\vec{K}\parallel[1\bar{1}0]$; $\vec{P}\parallel[1\bar{1}0]$, $\vec{K}\parallel[11\bar{2}]$; and $\vec{P}\parallel[11\bar{2}]$, $\vec{K}\parallel[1\bar{1}0]$. Changes in the reflection spectra were measured for the two polarizations during a stepwise application of uniaxial pressure up to about 2 kbar. Finally, the whole pressure was released to zero in order to check the recovery of the spectra to the original shape. The experimental results are shown in diagrams (a) of Figs. 2–6. Details of the observed spectra are discussed in Sec. III C in comparison with the theoretical results.

C. Comparison of Experimental and Theoretical Results

In Sec. II we described a theoretical framework for calculating the exciton states in uniaxially deformed CuCl. In this section we shall investigate how the present theory applies to the experimental results in explaining the characteristic features of the spectra.

Before going on to such discussions, we have to mention a problem associated with the quantitative analysis of the reflection spectra. In order to interpret precisely a reflection spectrum in terms of a microscopic theory of excitons (unperturbed by an external radiation field), we have to deal with a polariton problem with suitable boundary conditions at the crystal surface. Macroscopically, the behavior of polaritons is described by the dielectric tensor $\underset{\leftrightarrow}{\epsilon}(\omega,\vec{K})$ which is generally dependent on both ω and $\vec{K}$. Such a dielectric tensor which describes the polariton modes associated with excitons in uniaxially deformed CuCl is discussed in Sec. IV A. However, we shall find there that the polariton problem is too complicated to make a theoretical approach to the reflection spectrum. Moreover, we find that the spatial dispersion effect due to the k-linear dependence of $\epsilon(\omega,\vec{K})$ plays an essential role in the presently observed spectra in deformed CuCl. Consequently, we lose the foundation of analyzing the observed reflection spectra by means of the usual Kramers-Kronig transformation.

Thus since we have no feasible way at present to make a quantitative analysis of the results, we have to satisfy ourselves here with a semiquantitative comparison of the experimental and theoretical results. In the following, we shall consider separately the cases of the different experimental configurations.

1. $\vec{P}\parallel[001]$ *and* $\vec{K}\parallel[110]$

The spectra observed in this configuration [Fig. 2(a)] show the typical features of the effects of the uniaxial stress on excitons in CuCl in the most prominent way, as already mentioned in our previous reports.[6,7] Since a detailed interpretation

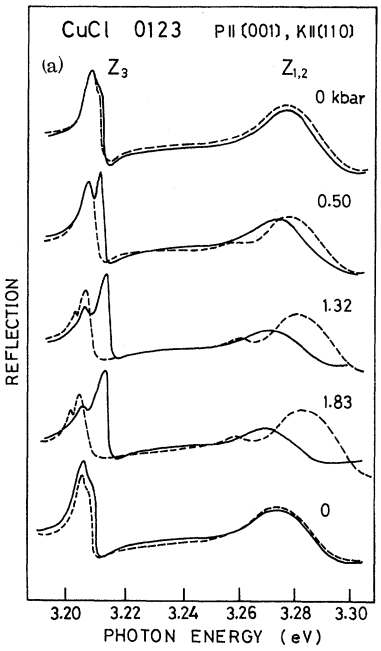

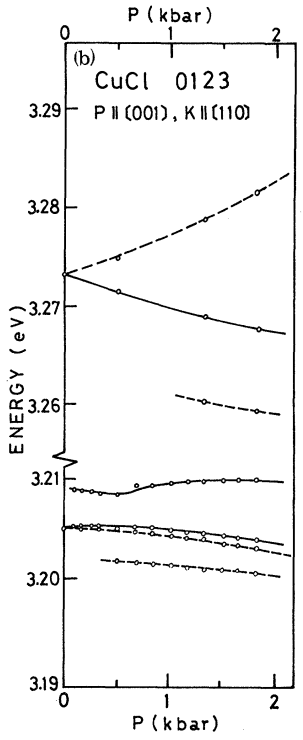

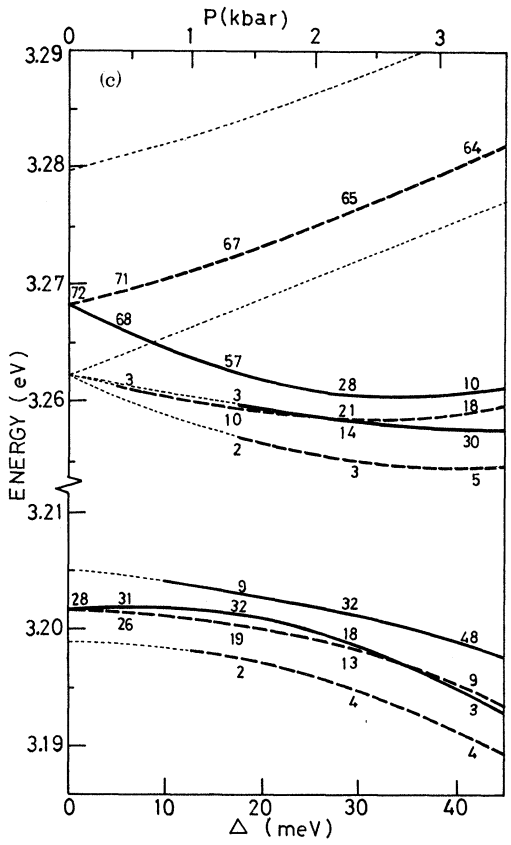

FIG. 2. Experimental and theoretical results for $\vec{P} \parallel [001]$ and $\vec{K} \parallel [110]$. (a) Observed change of the exciton reflection spectra with stress at 1.8 K. The solid and dashed curves represent the polarized components with $\vec{E} \parallel \vec{P}$ and $\vec{E} \perp \vec{P}$, respectively. (b) An experimental plot of the reflection peaks against applied pressure for $\vec{E} \parallel \vec{P}$ (solid lines) and $\vec{E} \perp \vec{P}$ (broken lines) polarizations. (c) Calculated exciton levels under stress plotted against the deformation energy $\Delta = D_1(e_{xx} - e_{zz}) = D_1(s_{11} - s_{12})P$. The parameters adopted are $D_1 = 1.2$ eV and $CK = 0.16$ eV. The corresponding scale for P is shown on the top of the figure. The solid and dashed lines represent the optically active levels polarized with $\vec{E} \parallel \vec{P}$ and $\vec{E} \perp \vec{P}$, respectively, while the dotted lines represent the optically inactive levels. Small figures on the curves indicate the relative oscillator strengths normalized to 100 for each polarization.

of the result has already been given, we shall only summarize here the important points relevant to the discussions to follow.

In the Z_3 exciton band, the original reflection structure shows a slight splitting into the $\vec{E} \parallel \vec{P}$ and $\vec{E} \perp \vec{P}$ components with increasing stress. In addition, a sharp new reflection peak appears for $\vec{E} \parallel \vec{P}$ on the high-energy side of the original Z_3 reflection band. This stress-induced peak grows up to an unusually strong reflection anomaly with $\vec{E} \parallel \vec{P}$ with increasing stress. Besides this, stress induces a much weaker but distinct reflection peak with $\vec{E} \perp \vec{P}$ on the low-energy side of the Z_3 peak. In the $Z_{1,2}$ band, the original structure splits into two polarized components with $\vec{E} \parallel \vec{P}$ and $\vec{E} \perp \vec{P}$, and a new structure is induced with stress for $\vec{E} \perp \vec{P}$ on the lower-energy side of the original $Z_{1,2}$ reflection peak. In order to show these stress-induced changes in the spectra, we have plotted in Fig. 2(b) the energies of the respective reflection peaks against the

applied stress. Since the reflection peaks do not correspond to the exact exciton resonance energies, this plot is only for a semiquantitative consideration before attaining a more rigorous method of analysis.

In a theoretical exciton matrix pertinent to this particular configuration, we have the deformation-potential constants D_1 and $D_0^c - D_0^v$ and the coefficient of the k-linear term, C, as the adjustable parameters to be determined from the experimental results. As for the deformation potentials, we estimate $D_1 = 1.2$ eV from the observed splitting of the $Z_{1,2}$ exciton as shown in Fig. 2(b). The sign of the figure should be positive from the observed polarization pattern of the splitting. On the other hand, we may assume that $D_0^c - D_0^v \approx 0$, since the center of gravity of the split components is almost independent of stress.

For the coefficient C of the stress-induced k-linear term, it is more difficult to make a reliable estimation. It has been definitely concluded in Refs. 6 and 7 that this parameter is not negligible, but plays an essential role in the observed spectra as seen from Fig. 2(a). In fact, if $C=0$, we would have no optically active mode induced on the high-energy side of the Z_3 exciton contrary to the experimental result. From the observed magnitude and energy position of the clamping point between the transverse (T) and longitudinal (L) modes of the Z_3 band, the combined parameter CK is estimated to be about 0.16 eV. The wave vector $\vec{K}$ of the exciton is considered to be equal to the photon wave vector $n\vec{K}_0$ in the medium. Here $\vec{K}_0$ is the wave vector of the photon in the vacuum, and is about 1.6×10^5 cm^{-1} at this energy. n is the refractive index in the resonant frequency region, and is tentatively assumed to be 10. The coefficient C is then estimated to be 1×10^{-7} eV cm. Further discussion regarding this parameter will be given later in Sec. IV C.

Results of the theoretical calculation resulting from this parameter fit are given in Fig. 2(c) which is to be compared with a semiquantitative experimental plot in Fig. 2(b). Here the calculated exciton energies associated with the Z_3 and $Z_{1,2}$ bands are plotted as a function of the deformation energy $\Delta = D_1(e_{xx} - e_{zz})$ in units of meV. The exciton energies at $\Delta = 0$ are fitted to the results by Staude.[11] The corresponding scale for the applied pressure P in kbar can be calculated from the estimated values of D_1 and the elastic compliance constants as shown on the top of the figure. Besides the eigenenergies for the exciton levels, the theory can predict the polarization and the relative intensities of the optically active exciton modes. The solid and dashed lines represent the optically active modes which are polarized with $\vec{E} \parallel \vec{P}$ and $\vec{E} \perp \vec{P}$, respectively. The calculated relative intensities of these modes are shown by figures on the curves which represent percents relative oscillator strengths, normalized to 100% for given polarization and stress. Optically inactive modes, including those with the oscillator strength less than 1%, are shown by dotted lines.

The essential features of this theoretical result pertinent to the interpretation of the experimental results are summarized as follows: From the deformation-potential constant D_1 which we have determined from the splitting of the $Z_{1,2}$ exciton, it is predicted for the Z_3 band that the $\vec{E} \parallel \vec{P}$ component of the transverse exciton (hereafter abbreviated as the T exciton) shifts towards higher energy, while the longitudinal exciton (the L exciton) to the lower energy. In the presence of the stress-induced k-linear term, even if quite small, a drastic change occurs near the crossover point of these two modes giving rise to a coupling between the L and T modes. The observed stress-induced reflection anomaly has been ascribed to such a clamping effect.[7] On the other hand, the $\vec{E} \perp \vec{P}$ component of the T exciton is split from the $\vec{E} \parallel \vec{P}$ component by a stress-exchange effect to lower energy. This mode couples with the triplet Γ_2 exciton lying on the low-energy side of it again by the stress-induced k-linear term. The observed appearance and its polarization are coincident with this theoretical prediction. These stress-induced couplings between the different exciton states are simply determined by the symmetries of these states under a particular deformation and can be easily predicted by a group-theoretical consideration. Moreover, a macroscopic approach to this problem leads us to an interpretation of the same phenomenon in terms of a macroscopic dielectric tensor $\epsilon(\omega, \vec{K})$ as discussed later in Sec. IV A.

As a summary of the comparison of the experimental and theoretical results in this configuration, we may conclude that the present theory can satisfactorily explain a number of peculiarities observed in this configuration. As a minor discrepancy with the theory, one notices in Fig. 2(a) that the observed strength of the L-T mixed mode in the Z_3 band is apparently much stronger than the theoretical prediction. The explanation for this effect will have to be sought in the polariton problem involved in the interpretation of the reflection spectra, rather than a different choice of the constant C.

2. $\vec{P} \parallel [001]$ *and* $\vec{K} \parallel [100]$

In this and following configurations, the experimental results are shown only for the observed spectra. Experimental plots similar to Fig. 2(b) become quite ambiguous, in particular for the complicated structures observed in the $Z_{1,2}$ band, so that we shall satisfy ourselves to make a direct inspection of the observed spectra in comparison

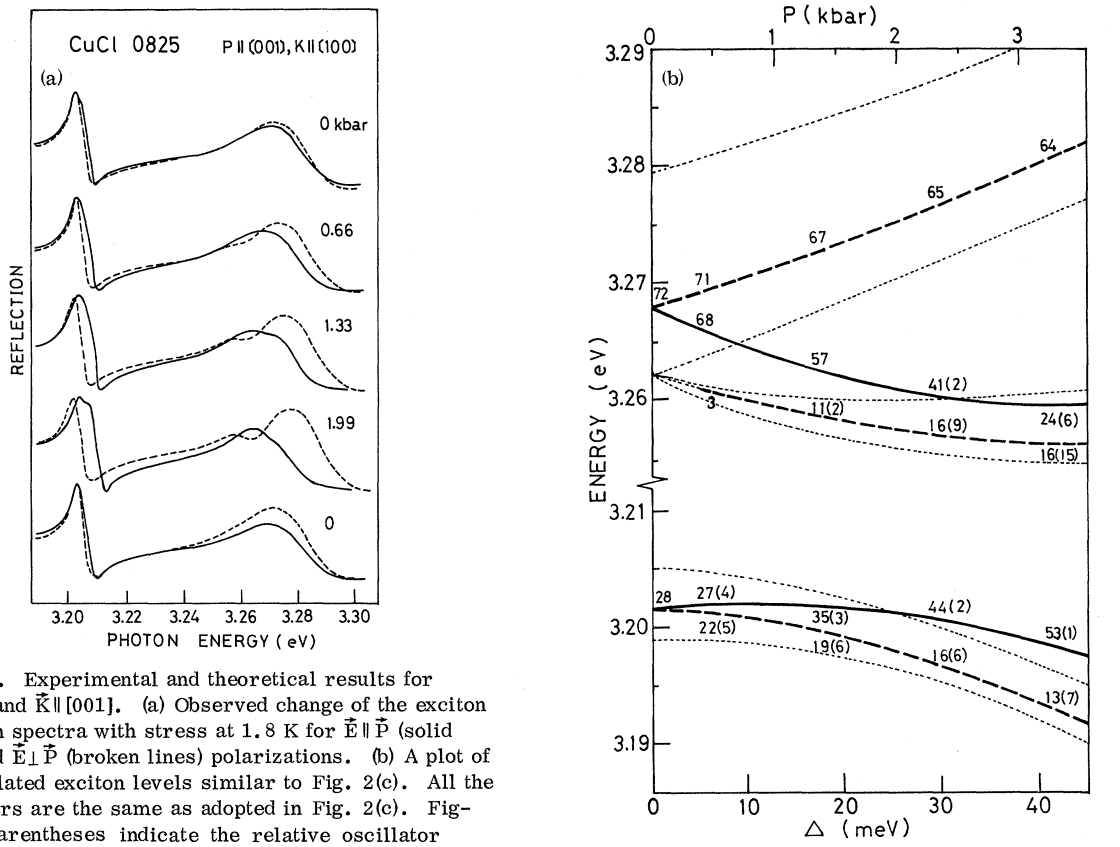

FIG. 3. Experimental and theoretical results for $\vec{P} \parallel [001]$ and $\vec{K} \parallel [001]$. (a) Observed change of the exciton reflection spectra with stress at 1.8 K for $\vec{E} \parallel \vec{P}$ (solid lines) and $\vec{E} \perp \vec{P}$ (broken lines) polarizations. (b) A plot of the calculated exciton levels similar to Fig. 2(c). All the parameters are the same as adopted in Fig. 2(c). Figrues in parentheses indicate the relative oscillator strengths of the weaker polarization components in the incompletely polarized exciton states.

with the theoretical calculation.

The experimental and theoretical results are represented in Figs. 3(a) and 3(b), respectively. In the observed spectra, the behavior of the $Z_{1,2}$ band is quite similar to case 1 except that the reflection peaks are not completely polarized in either $\vec{E} \parallel \vec{P}$ or $\vec{E} \perp \vec{P}$ directions. On the other hand, we immediately notice that the Z_3 band behaves quite differently from the case of $\vec{P} \parallel [001]$ and $\vec{K} \parallel [110]$. Strong anomalies due to the L-T mixed mode exciton and the stress-induced triplet Γ_2 exciton are completely absent in this configuration.

The theoretical result to be compared with these spectra is calculated with all the parameters estimated in the preceding case, and is shown in Fig. 3(b). The essential difference from case 1 arises from the fact that the stress-induced k-linear term couples the two T modes of the Z_3 and $Z_{1,2}$ bands and also the L mode with the triplet Γ_2 exciton in the Z_3 band. Due to the absence of the L-T coupling in this configuration, there is no clamping effect in contrast to the preceding case, which is in excellent agreement with the experimental result. The absence of the stress-induced Γ_2 triplet exciton in the observed spectra for this configuration also confirms this prediction. Due to the coupling between the T modes, polarizations of the optically active modes are not complete in this configuration. The figures in the brackets represent the relative oscillator strengths of the weaker components. For example, the Z_3 exciton polarized with $\vec{E} \perp \vec{P}$ gets a considerable amount of the $\vec{E} \parallel \vec{P}$ component as a result of such a coupling. This explains the coinciding peaks in the observed $\vec{E} \perp \vec{P}$ and $\vec{E} \parallel \vec{P}$ spectra. On the other hand, as the exciton polarized with $\vec{E} \parallel \vec{P}$ obtains only a slight amount of the $\vec{E} \perp \vec{P}$ component, it cannot be observed at the proper energy position by the light with polarization $\vec{E} \perp \vec{P}$.

3. $\vec{P} \parallel [111]$ *and* $\vec{K} \parallel [1\bar{1}0]$

In this configuration, the relevant exciton matrix contains the deformation-potential constant D_2 and another coefficient B for the stress-induced k-linear term as the adjustable parameters. These parameters are estimated in a similar way as made in case 1. From observed stress splitting of the $Z_{1,2}$ exciton, we estimate $D_2 = -2.4$ eV. As for B, we tentatively assume $B \approx 10^{-7}$ eV cm. The stress-induced k-linear term in this configuration gives rise to a coupling of the L mode with the $\vec{E} \parallel \vec{P}$ component of the T mode and a coupling of the triplet Γ_2 exciton with the $\vec{E} \perp \vec{P}$ component of the T mode.

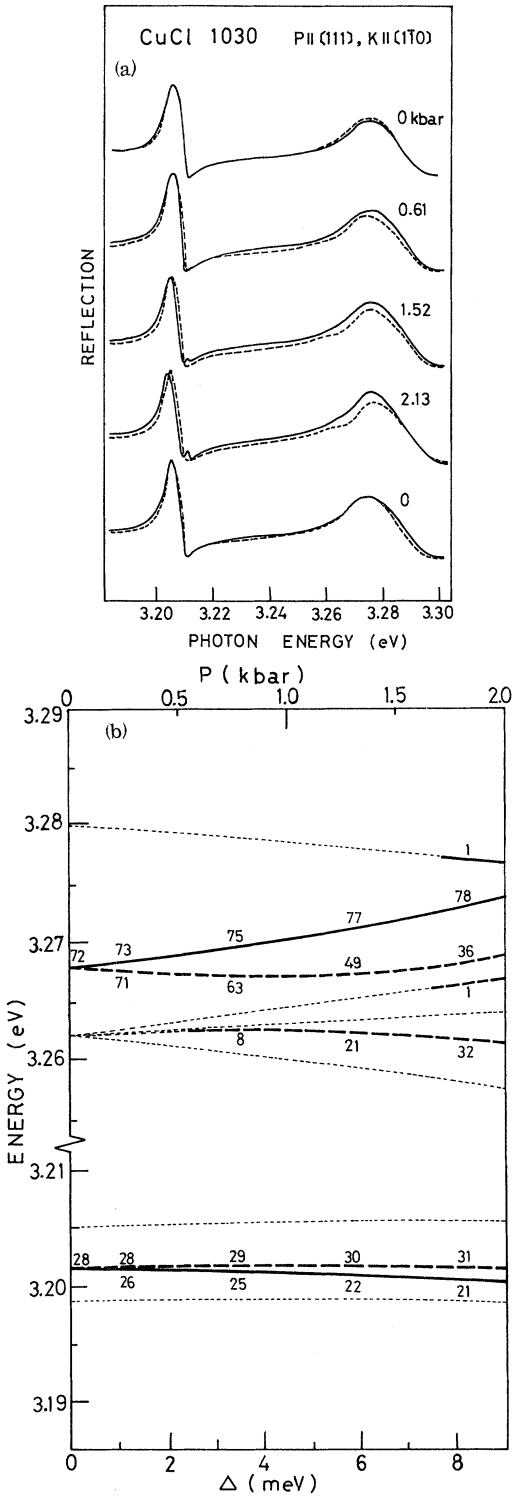

FIG. 4. Experimental and theoretical results for $\vec{P}\parallel[111]$ and $\vec{K}\parallel[1\bar{1}0]$. (a) Observed change of the exciton reflection spectra with stress at 1.8 K for $\vec{E}\parallel\vec{P}$ (solid lines) and $\vec{E}\perp\vec{P}$ (broken lines) polarizations. (b) A plot of the calculated exciton levels against $\Delta = D_2 e_{xy} = -\frac{1}{3}D_2 S_{44} P$. The parameters used are $D_2 = -2.4$ eV and $BK = 0.16$ eV.

However, in contrast to case 1, the energy separations between the coupling modes are all increased with stress, as seen in Fig. 4(b), so that the effect of the mode coupling is expected to be too small to be observable.

As for the $Z_{1,2}$ band, the theory predicts complicated structures for the $\vec{E}\perp\vec{P}$ component originating from a coupling of the $\vec{E}\perp\vec{P}$ component of the $Z_{1,2}$-T mode with the triplet $\Gamma_{3,4}$ excitons. Such structures are indeed observed in the experimental result shown in Fig. 4(a).

4. $\vec{P}\parallel[1\bar{1}0]$ *and* $\vec{K}\parallel[11\bar{2}]$

All parameters involved in the exciton matrix have been estimated in the preceding cases 1 and 3, so that we can check the validity of the theory in the following two cases. First, we consider the case of $\vec{P}\parallel[1\bar{1}0]$ and $\vec{K}\parallel[11\bar{2}]$, the experimental result of which is shown in Fig. 5(a).

A remarkable feature of the spectra in this configuration is the sharp reflection peak appearing on the high-energy side of the Z_3 band for $\vec{E}\perp\vec{P}$. According to the present theory, the origin of this peak is interpreted as follows: By applying stress $\vec{P}\parallel[1\bar{1}0]$, the cubic symmetry of the zinc-blende CuCl is reduced to the monoclinic one with the principal axis along the [001] direction. For $\vec{K}\parallel[11\bar{2}]$, the $\vec{K}$ vector of the incident light makes an angle of 35° from this principal axis. Such an off-axis incidence of light gives rise to a L-T mode mixing both in the Z_3 and $Z_{1,2}$ bands through the electron-hole exchange interaction. The stress-induced k-linear term also contributes to the same coupling as well as to a slight coupling between the triplet Γ_2 exciton and the $\vec{E}\parallel\vec{P}$ component of the Z_3 exciton. However the contribution of the stress-induced k-linear term is predicted to be much smaller than the effect of the off-axis incidence. Thus the observed stress-induced sharp anomaly in the Z_3 band is considered to be dominantly due to the off-axis incidence effect characteristic to the low symmetry of this configuration. The theoretical result shown in Fig. 5(b) is thus in qualitative agreement with the observed spectra.

5. $\vec{P}\parallel[11\bar{2}]$ *and* $\vec{K}\parallel[1\bar{1}0]$

The symmetry is the lowest, in this case, among the experimental configurations adopted. The stress-induced appearance of the L-T mixed mode in the Z_3 band as seen in Fig. 6(a) is likewise attributed to the effect of off-axis incidence as in the preceding case. Complicated structures of the $Z_{1,2}$ band are clearly observable. These observed features are in good accord with the theoretical prediction shown in Fig. 6(b).

IV. DISCUSSION

A. Phenomenological Interpretation in Terms of Stress-Dependent Gyrotropic Dielectric Tensor

In Secs. I–III, we have given a microscopic explanation of the phenomena in terms of the exciton states under stress, where possible couplings between different exciton states and their polarization characteristics have been understood directly on the basis of the effective-mass theory of excitons with the stress-induced k-linear terms taken into account. We now show below that the same results can be derived in a qualitative sense by investigating the behavior of the macroscopic dielectric tensor with the aid of symmetry considerations.

Dielectric response of excitons, in particular with the Z_3 exciton in deformed CuCl kept in mind, is described by a dielectric tensor $\epsilon(\omega, \vec{K})$, or else more conveniently by its inverse $\epsilon^{-1}(\omega, \vec{K})$. We expand this tensor in powers of the wave vector $\vec{K}$ as

$$\epsilon_{ij}^{-1}(\omega, \vec{K}) = \epsilon_{ij}^{-1}(\omega) + i\delta_{ijl}(\omega)K_l , \tag{8}$$

neglecting terms higher than first order in $\vec{K}$.[15,16]

The coefficient δ_{ijl} of the k-linear term is required to be antisymmetric with respect to the interchange of the first two indices $\delta_{ijl} = -\delta_{jil}$, by the symmetry relation $\epsilon_{ij}^{-1}(\omega, -\vec{K}) = \epsilon_{ji}^{-1}(\omega, \vec{K})$ of the dielectric constant. One can therefore write $\delta_{ijl}K_l = e_{ijm}f_{ml}K_l = e_{ijm}f_m$, where e_{ijm} is the antisymmetric pseudotensor of rank three.[15] With use of this vector $\vec{f}$, called the gyration vector, the electric field $\vec{E}$ in the medium is connected to the electric displacement vector $\vec{D}$ by

$$\vec{E} = \epsilon^{-1}(\omega)\cdot\vec{D} - i\vec{f}\times\vec{D} . \tag{9}$$

In a medium with nonzero $\vec{f}$, the $\vec{E}$ vector has a component $-i\vec{f}\times\vec{D}$ which is perpendicular to both $\vec{f}$ and $\vec{D}$. The normal mode of propagation for $\vec{E}$ is then determined by the symmetry of $\epsilon_{ij}^{-1}(\omega)$ and by the direction of $\vec{f}$ with respect to the $\vec{K}$ vector. For simplicity we shall consider the case in which $\epsilon_{ij}^{-1}(\omega)$ is diagonal and assume that $\vec{f} \neq 0$. If $\vec{f} \parallel \vec{K}$, the $\vec{E}$ vector is composed of two mutually perpendicular transverse components. Macroscopically, this leads to the optical activity of the medium. From a microscopic point of view, this corresponds to a situation in which a coupling occurs between the two T modes of an exciton by virtue of the spatial dispersion linear in $\vec{K}$. On the other hand, if $\vec{f} \perp \vec{K}$, the second term of Eq. (9) represents a longitudinal component of $\vec{E}$ (since $\vec{D} \perp \vec{K}$ always), while the first term is of purely transverse nature. A microscopic interpretation of this situation is a coupling of the L and T modes associated with an exciton via a k-linear effect.

Generally, the relative orientation of $\vec{f}$ with respect to $\vec{K}$ is determined by the symmetric pseudo-

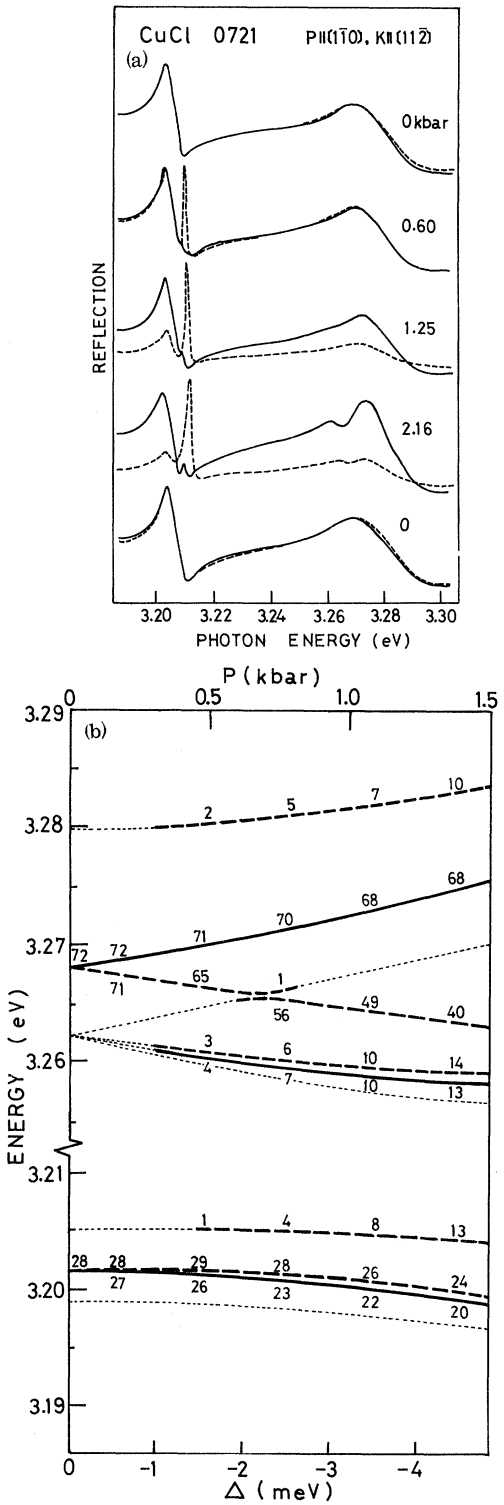

FIG. 5. Experimental and theoretical results for $\vec{P} \parallel [1\bar{1}0]$ and $\vec{K} \parallel [11\bar{2}]$. (a) Observed change of the exciton reflection spectra with stress at 1.8 K for $\vec{E} \parallel \vec{P}$ (solid lines) and $\vec{E} \perp \vec{P}$ (dashed lines) polarizations. (b) A plot of the calculated exciton levels against $\Delta = D_1 e_{xx} = -\frac{1}{2}D_1(s_{11}+s_{12})P$. All the parameters used are the same as adopted in Figs. 2(c) and 4(b).

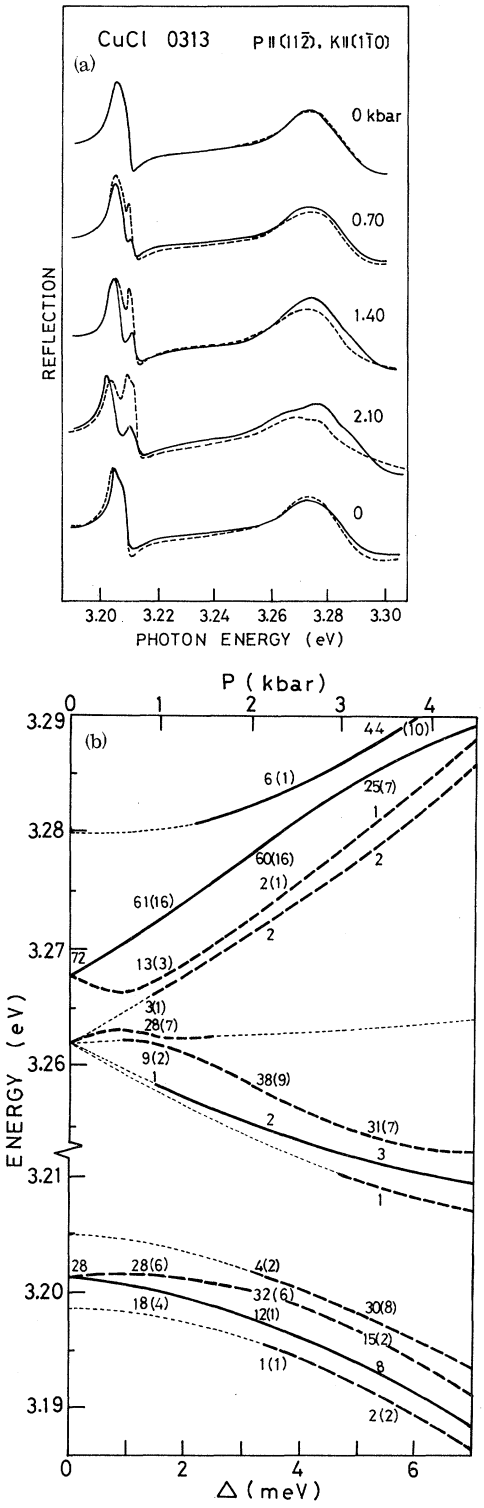

FIG. 6. Experimental and theoretical results for $\vec{P} \parallel [11\bar{2}]$ and $\vec{K} \parallel [1\bar{1}0]$. (a) Observed change of the exciton reflection spectra with stress at 1.8 K for $\vec{E} \parallel \vec{P}$ (solid lines) and $\vec{E} \perp \vec{P}$ (dashed lines) polarizations. (b) A plot of the calculated exciton levels against $\Delta = D_1 e_{xx} = -\frac{1}{6} D_1 (5s_{12} + s_{11}) P$. All the parameters used are the same as adopted in Figs. 2(c) and 4(b).

tensor f_{ij}. Symmetry properties of this gyration tensor f_{ij} are determined solely by the crystal symmetry as has been investigated by several authors.[15,17] We investigate here the possible properties of the gyrotropic tensor in the case of CuCl.

In undeformed CuCl, the dielectric tensor is isotropic and the gyration tensor f_{ij} vanishes because of the T_d symmetry. Then, we consider the case where an external stress is applied along the [001] axis (z). The point symmetry of the crystal is reduced from T_d to D_{2d}. In this symmetry, nonvanishing elements of the gyration tensor f_{ij} are solely $f_{xx} = -f_{yy} \equiv f$. (Here the x and y axes are taken along the crystallographic [100] and [010] axes, respectively.) Then the tensor $\epsilon_{ij}^{-1}(\omega, \vec{K})$ is written as a function of $(\omega, \vec{K})$ and of the external pressure $\vec{P}$ as

$$\epsilon_{ij}^{-1}(\omega, \vec{K}, \vec{P}) = \begin{vmatrix} \epsilon_{\perp}^{-1}(\omega, \vec{P}) & 0 & if(\vec{P})K_y \\ 0 & \epsilon_{\perp}^{-1}(\omega, \vec{P}) & if(\vec{P})K_x \\ -if(\vec{P})K_y & -if(\vec{P})K_x & \epsilon_{\parallel}^{-1}(\omega, \vec{P}) \end{vmatrix} . \tag{10}$$

In this expression, the difference of $\epsilon_{\perp}^{-1}$ and $\epsilon_{\parallel}^{-1}$ arises from the stress-induced splitting of the T modes of the relevant exciton band, specifically from the stress-exchange splitting for the Z_3 exciton. The coefficient f is the nonzero element of the stress-induced gyration tensor and is considered to be proportional to the applied pressure $\vec{P}$ for a small $\vec{P}$.

A microscopic expression for the dielectric tensor which describes the dielectric response of the Z_3 excitons will be given in the Appendix. It is shown that the phenomenological dielectric function is well founded on the microtheoretical basis. Then we can proceed with a phenomenological consideration on the basis of the inverse dielectric tensor described above. In the case of $\vec{P} \parallel [001]$ and $\vec{K} \parallel [110]$, the gyration vector $\vec{f}$ is immediately found to lie along the $[1\bar{1}0]$ direction, so that $\vec{f} \perp \vec{K}$ in this configuration. According to the consideration mentioned above, a coupling should occur between the $\vec{E} \parallel \vec{P}$ transverse component and the L component of the $\vec{E}$ vector, whereas the $\vec{E} \perp \vec{P}$ component remains a pure T mode. (The corresponding microscopic theory described in Sec. III C predicts a mixing of this mode with the pure triplet exciton. However the present phenomenological theory has nothing to do with the triplet excitons for which the dipole matrix elements vanish.) As a result, we find that the phenomenological theory leads us to just the same coupling and polarization scheme as has actually been observed in this configuration.

Next we consider the case of $\vec{P} \parallel [001]$ and

$\vec{K} \parallel [100]$. The gyration vector in this configuration is found to be parallel to $\vec{K}$, so that we can expect a coupling between the two T modes through the k-linear effect. The normal modes of propagation of the $\vec{E}$ vector are two oppositely rotating elliptic modes with mutually perpendicular major axes. Again we find a correct correspondence between this phenomenological picture and the microscopic theory which predicts the stress-induced coupling of the two T modes via k-linear term.

Similar phenomenological considerations are valid for other experimental configurations as well. When the applied stress reduces the crystal symmetry lower than that of an axial symmetry, the tensor $\epsilon^{-1}(\omega)$ contains off-diagonal elements in zeroth order of $\vec{K}$. The resulting optical anisotropy causes a L-T mode mixing for an off-axis incidence of $\vec{K}$, corresponding to the situation we have discussed for cases 4 and 5 in Sec. III C.

As a summary, we can rephrase the present phenomena as stress-induced optical gyrotropy in CuCl. Naturally such a simple macroscopic picture cannot tell us anything about the microscopic exciton energy spectrum, including the possible clamping effect and participation of the pure triplet excitons. Nevertheless, such a macroscopic view will be quite useful in the future study of excitons under stress, not merely as an instructive alternative of the interpretation. In the first place, such a macroscopic consideration is expected to lead us to a more detailed understanding of the polariton problem which is required for quantitative analysis of the reflection spectra. Further, it will provide us with an interesting case of crystal optics, in general, where an optical activity in crystal is directly correlated with a microscopic behavior of excitons. Another point to be stressed is the generality of our macroscopic considerations which depend solely on the symmetry of the crystal and of the experimental configuration. Besides, although we have kept excitons in mind, the theory remains valid for any other polarization waves in a crystal, such as optical modes of lattice vibration. One can therefore expect just the same effects in the infrared spectra as we observed for excitons. It will perhaps be very interesting to detect a possible similar anomaly in the optic lattice vibrations and investigate its microscopic origin.

B. Possible Effects of Off-Axis Incidence of Light

When the $\vec{K}$ vector of the incident light is not oriented along one of the principal axes of the dielectric tensor, there occurs a L-T mode mixing in the zeroth order of $\vec{K}$. This problem of an off-axis incidence has been discussed by Hopfield and Thomas.[18] They developed a continuum theory of the dielectric property due to the direct excitons in a wurtzite crystal and showed a dependence of the mixed mode energy upon the angle of incidence from the principal axis. In this connection we may note that the present theory extended in Sec. II C is actually a general theory which includes the effects of such an off-axis incidence from a microscopic point of view. Here, the wave vector of the exciton and the external uniaxial stress can be taken in arbitrary directions. For example, in the configurations 4 and 5 discussed in Sec. II C, the external stress reduces the cubic symmetry to the monoclinic and triclinic ones, respectively. The resulting L-T mode mixing in the Z_3 exciton band is dominantly due to the effect of an off-axis incidence of light in the deformed crystal. In microscopic terms this has been described as a combined effect of the stress and the electron-hole exchange interaction.

Since such an effect of the off-axis incidence is of the zeroth order in $\vec{K}$ and hence is much more effective in producing an appreciable mixing of the L and T modes, one might suspect that the anomalous L-T mixing observed in configuration 1 might also be caused, more or less, by a possible off-axis incidence arising from a slight misalignment of the experimental geometry, rather than by the stress-induced k-linear term. However, this possibility can be eliminated for the following three reasons: First, the off-axis incidence never gives rise to a mixing of the T and triplet Γ_2 excitons, which is simultaneously detected in this configuration. The second reason comes from the particular symmetry of the Z_3 exciton. If we neglect small stress-induced k-linear terms, the submatrix corresponding to the (Γ_7, Γ_6) pair in the exciton matrix is completely diagonal, and consequently there is no direct coupling in the (Γ_7, Γ_6) excitons even for the off-axis incidence. A possible coupling between the L and T modes can only occur through an indirect interaction via the (Γ_8, Γ_6) exciton states. The magnitude of this interaction is roughly estimated as $(\Delta_L \Delta/3\lambda)\sin\theta$. Here θ is the angle of deviation of $\vec{K}$ from the [110] direction, which is estimated to be less than 5° in the present measurement. Since the deformation energy $\Delta = D_1 \times (e_{xx} - e_{zz})$ defined in Sec. III C will be at most about 20 meV at the largest stress in the measurement, the possible interaction energy is too small to explain the observed L-T mode mixing of the Z_3 exciton band. Finally, the effect of the off-axis incidence cannot account for the observed difference in the configurations of $\vec{K} \parallel [110]$ and $\vec{K} \parallel [100]$ for the same stress $\vec{P} \parallel [001]$, whereas the stress-induced k-linear term can successfully explain it.

As a summary of the discussion above, an anomalous L-T mixing observed in the Z_3 band for $\vec{P} \parallel [001]$ and $\vec{K} \parallel [110]$ is conclusively ascribed to the stress-induced k-linear term. On the other hand, the same L-T mixed mode observed in the

configurations with lower symmetry is considered to be dominantly due to the effect of an off-axis incidence. In fact, in the latter case the calculated intensities of the L-T mixed mode are almost unchanged even if we neglect the stress-induced k-linear terms in the exciton matrix.

C. Coefficients B and C of Stress-Induced k-Linear Terms

In Sec. III C, the coefficients of the stress-induced k-linear terms, B and C, were estimated as $\sim 10^{-7}$ eV cm from a semiquantitative comparison of the experimental and theoretical results. Though this estimation should be regarded as only a crude one in the order of magnitude, it will be helpful to see if this magnitude is consistent with the actual energy-band structure of CuCl. A theoretical evaluation of C has already been discussed in the previous work.[7] Here we shall provide an additional discussion on the magnitude of the coefficients B and C.

According to the second-order perturbation calculation of a bilinear term in $\vec{k}\cdot\vec{p}$ and strain, these coefficients are expressed as follows:

$$B \simeq i\frac{\hbar}{m}\left(-\frac{\langle b_x(\Gamma_5^u)|V_{yz}|s(\Gamma_1^c)\rangle\langle s(\Gamma_1^c)|p_y|b_y(\Gamma_5^u)\rangle}{E(\Gamma_5^u)-E(\Gamma_1^c)}+\frac{\langle b_y(\Gamma_5^u)|V_{yz}|b_z(\Gamma_5^l)\rangle\langle b_z(\Gamma_5^l)|p_y|b_x(\Gamma_5^u)\rangle}{E(\Gamma_5^u)-E(\Gamma_5^l)}\right.$$
$$\left.+\frac{\langle b_x(\Gamma_5^u)|p_x|b_{2x^2-y^2-z^2}(\Gamma_3)\rangle\langle b_{2x^2-y^2-z^2}(\Gamma_3)|V_{xz}|b_y(\Gamma_5^u)\rangle}{E(\Gamma_5^u)-E(\Gamma_3)}\right), \quad (11a)$$

$$C \simeq i\frac{\sqrt{2}\hbar}{m}\frac{\langle b_x(\Gamma_5^u)|V_{x^2-y^2}|b_x(\Gamma_5^l)\rangle\langle b_x(\Gamma_5^l)|p_z|b_y(\Gamma_5^u)\rangle}{E(\Gamma_5^u)-E(\Gamma_5^l)}. \quad (11b)$$

Here $V_{x^2-y^2}$ and V_{xy} are the crystal potentials which are conjugates to the strains $(1/\sqrt{2})(e_{xx}-e_{yy})$ and e_{xy}, respectively; Γ_5^l and Γ_3 represent the lower valence bands[8] lying about 3 and 0.7 eV below the upper valence band Γ_5^u, respectively; and the b's are the respective valence-band Bloch functions. $s(\Gamma_1^c)$ is the Bloch function of the Γ_1^c conduction band.

A theoretical calculation of B and C from expressions given above is, however, not feasible at present on account of the lack of the quantitative knowledge of the matrix elements involved in Eqs. (11). Instead, we shall satisfy ourselves to make an inference on the magnitude of these coefficients in comparison with the previously known k-linear terms in wurtzite II-VI crystals.

The intrinsic k-linear term which appears in the off-diagonal element of the Γ_7 valence band of wurtzite CdS and ZnO has been discussed by Hopfield[19] and by Mahan and Hopfield,[20] and the coefficient C (in Hopfield's notation) for CdS has been estimated to be 6×10^{-9} eV cm. (It seems to us that this is possibly somewhat overestimated.) If we regard the wurtzite lattice as a uniaxially deformed zinc-blende crystal according to a quasicubic model, such an intrinsic k-linear term in wurtzite crystal is related to the stress-induced k-linear term in deformed zinc blende, and the coefficient C of Hopfield is approximately expressed either as Be_{xy} (for $\lambda \gtrsim D_2 e_{xy}$) or as $(\lambda/D_2 e_{xy})Be_{xy}$ (for $\lambda \ll D_2 e_{xy}$). Since $e_{xy}\sim 3\times10^{-3}$ at an external pressure of about 1.5 kbar in CuCl, the resulting coefficient C will be about 3×10^{-10} eV cm, assuming $B\approx 10^{-7}$ eV cm as estimated before. This magnitude is nearly comparable with the estimation in CdS, which justifies the evaluation of the coefficient B.

V. CONCLUSION

It has been established that stress-induced k-linear terms play an essential role in the anomalous exciton spectra of uniaxially deformed CuCl. In particular, an extraordinary reflection peak observed on the high-energy side of the Z_3 exciton band for $\vec{P}\parallel[001]$ and $\vec{K}\parallel[110]$ is conclusively ascribed to the strong coupling between the L and T modes near the crossover point via the stress-induced k-linear term. A small stress-induced k-linear dispersion of the exciton is sufficient to produce a drastic change in the Z_3 reflection spectra as observed. The same exciton matrix formalism, which takes the spin-exchange, strain, and the stress-induced k-linear terms into account, is found to be valid in explaining the characteristic features of the exciton spectra observed in other experimental configurations as well. When the external stress lowers the crystal symmetry further, the effect of an off-axis incidence is found to predominate in the L-T mode mixing over the stress-induced k-linear effect. All of these effects can be simultaneously taken into account in the general exciton matrix formalism presented here.

From a macroscopic point of view, these phenomena can be regarded as being due to a stress-induced optical gyrotropy in the medium. A stress-dependent dielectric tensor with a k-linear spatial dispersion provides a phenomenological interpretation of the behavior of exciton spectra under

stress. Further, this dielectric tensor has been shown to be derivable directly from the explicit exciton wave functions under stress. The present phenomena provide us with an interesting case for the microscopic study of the optical gyrotropy in crystals.

Although in our present study comparison of theory and experiment is restricted to a semiquantitative extent because of difficulties in directly analyzing the reflection spectra observed, approximate estimations have been made for the deformation potential constants D_1 and D_2 and for the coefficients of the stress-induced k-linear terms: $D_1 = 1.2$ eV, $D_2 = -2.4$ eV, and $B, C \approx 10^{-7}$ eV cm.

Among the remaining problems left for future work, first we shall have to deal with the polariton problem associated with the excitons in deformed CuCl. Complications arise from the fact that various couplings are caused between the exciton levels by the combined effect of the strain, strain-induced k-linear term, and spin exchange. The problem therefore does not seem to be easily handled at the present stage, despite its importance for a quantitative understanding of the reflection spectra observed.

Finally, we would like to emphasize the uniqueness of the effects of uniaxial stress on excitons, as investigated here, because they reveal several new aspects of excitons in ionic crystals which have not been pursued on purpose. Cuprous halides are supposed to be some of the most suitable materials for such a study. We are now extending the same measurements on CuBr and CuI crystals.

ACKNOWLEDGMENTS

The authors are grateful to Dr. O. Akimoto for valuable discussions and to Professor S. Shionoya and his colleagues for making the experimental facilities available to us. Part of this work is financially supported by the Nishina Memorial Foundation and by the Mitsubishi Science Foundation.

APPENDIX

Here, we indicate a microscopic derivation of the dielectric tensor, thereby giving a substantiation to the phenomenological considerations developed in Sec. IV A. A general expression for the contribution of excitons to the dielectric tensor has been derived in Ref. 15 as

$$\epsilon_{ij}(\omega,\vec{K}) = \left(1 - \frac{4\pi N e^2}{V m \omega^2}\right)\delta_{ij} - \frac{4\pi c^2}{V\hbar\omega^2} \times \sum_s \left(\frac{M^i_{0;-Ks}(\vec{K}) M^j_{-Ks;0}(-\vec{K})}{\omega - \omega_s(\vec{K})} - \frac{M^i_{Ks;0}(\vec{K}) M^j_{0;Ks}(-\vec{K})}{\omega + \omega_s(-\vec{K})} \right) \tag{A1}$$

in terms of the matrix elements of an operator

$$\vec{M} = -(e/2mc)\sum_\alpha (\vec{P}^\alpha e^{i\vec{K}\cdot\vec{r}_\alpha} + e^{i\vec{K}\cdot\vec{r}_\alpha}\vec{P}^\alpha) . \tag{A2}$$

Here $(\vec{K}, s)$ refers to a mechanical (uncoupled to any electric field) exciton with the wave vector $\vec{K}$, eigenfrequency $\omega_s(\vec{K})$, and quantum number s, while $\vec{P}^\alpha$ and $\vec{r}_\alpha$ are the momentum and position vectors of the αth electron, respectively. N is the total number of electrons and V the volume of the crystal.

In applying this expression to a calculation of the dielectric tensor of deformed CuCl under consideration, we take for $(\vec{K}, s)$ only the Z_3 exciton states explicitly and assume that all other contributions are included in a dielectric tensor $\epsilon'_{ij}(\omega)$. Using the basis for the Z_3 excitons with the k-linear dispersion as derived in Sec. II C, the calculation was made for $\vec{P} \parallel [001]$. For this particular stress direction, the dielectric tensor becomes as follows to first order in $\vec{K}$:

$$\epsilon_{ij}(\omega,\vec{K}) = \epsilon_{ij}(\omega)\delta_{ij} + i\gamma_{ijl}(\omega)K_l , \tag{A3}$$

where

$$\epsilon_\perp(\omega) \equiv \epsilon_{xx} = \epsilon_{yy} = \epsilon'_\perp - \frac{4\pi e^2}{m^2\hbar\omega^2}|F(0)|^2 \frac{A_1 P^2}{\omega - \omega_1(0)} , \tag{A4}$$

$$\epsilon_\parallel(\omega) \equiv \epsilon_{zz} = \epsilon'_\parallel - \frac{4\pi e^2}{m^2\hbar\omega^2}|F(0)|^2 \frac{A_2 P^2}{\omega - \omega_2(0)} , \tag{A5}$$

and

$$\gamma_{xz,y} = \gamma_{yz,x} = -\gamma_{zx,y} = -\gamma_{zy,x} \equiv g(\omega) , \tag{A6}$$

with

$$g(\omega) = \frac{4\pi e^2}{m^2\hbar\omega^2}|F(0)|^2 \left[\frac{(A_1A_2)^{1/2}A_3 P^2}{(A_1 - A_2)\Delta_T} \left(\frac{1}{\omega - \omega_1(0)} - \frac{1}{\omega - \omega_2(0)} \right) + PQ\left(\frac{A_1}{\omega - \omega_1(0)} - \frac{A_2}{\omega - \omega_2(0)} \right) \right] . \tag{A7}$$

In these expressions, $\hbar\omega_1(0)$ and $\hbar\omega_2(0)$ are the energies of the mechanical Z_3 excitons at $\vec{K} = 0$ in deformed CuCl given by

$$\hbar\omega_i(0) = A_i\Delta_T + [E_g - E(\Gamma_7) - E_b] \quad \text{for } i = 1, 2 .$$

E_b is the exciton binding energy, and E_g the energy difference between the Γ_1 and Γ_5 bands of the undeformed crystal. P and Q are the dipole and quadrupole moments, respectively, given by

$$P = \frac{V}{\Omega}\int_\Omega b_s^* P_x b_x d\tau, \quad Q = \frac{V}{\Omega}\int_\Omega b_s^* P_x y b_z d\tau ,$$

where b_s and $b_{x,y,z}$ stand for the Bloch functions of the Γ_1 and Γ_5 bands, respectively, and Ω the volume of the unit cell. Finally, parameters A_1, A_2, and A_3 are defined as

$$A_1=\left(\frac{\lambda}{3E(\Gamma_7)-\lambda}\right)^2\left(1+\frac{2\lambda^2}{[3E(\Gamma_7)-\lambda]^2}\right)^{-1},$$

$$A_2=\left(1+\frac{2\lambda^2}{[3E(\Gamma_7)-\lambda]^2}\right)^{-1}, \tag{A8}$$

$$A_3=C\,\frac{\Delta}{D_1}\left(\frac{\lambda}{3E(\Gamma_7)-\lambda}\right)A_2,$$

where $E(\Gamma_7)$ is the energy of the uppermost Γ_7 valence band in the deformed crystal as given by

$$E(\Gamma_7)=\tfrac{1}{2}(\Delta+\tfrac{1}{3}\lambda)+\tfrac{1}{2}(\Delta^2-\tfrac{2}{3}\lambda\Delta+\lambda^2)^{1/2}.$$

The meaning of the other parameters is same as used in the text.

In expression (A7) for $g(\omega)$, the first term in the large parentheses originates from the k-linear dispersion of the Z_3 exciton, while the second term comes from the quadrupole moment of the exciton which can exist irrespective of the k-linear dispersion of the exciton. However, the ratio of the first to the second term is estimated as

$$\frac{(A_1A_2)^{1/2}A_3P^2}{(A_1-A_2)\Delta_T PQ}\approx\left(\frac{P}{Q}\right)\frac{C\lambda}{D_1}\geq 10,$$

so that we may neglect the latter contribution.

We note that the dielectric tensor (A3) has the same structure as the inverse dielectric tensor (10) deduced in the text from symmetry considerations to first order in K, as it should. We thus have given a microscopic foundation for the macroscopic considerations on the optical gyrotropy developed in Sec. IV A.

[1]For example, D. G. Thomas, J. Appl. Phys. 32, 2298 (1961).

[2]Y. Onodera and Y. Toyozawa, J. Phys. Soc. Japan 22, 833 (1967).

[3]T. Koda and D. W. Langer, Phys. Rev. Letters 20, 50 (1968); O. Akimoto and H. Hasegawa, *ibid.* 20, 916 (1968).

[4]D. W. Langer, R. N. Euwema, K. Era, and T. Koda, Phys. Rev. B 2, 4005 (1970); G. L. Bir, G. E. Pikus, L. G. Suslina, and D. L. Fedorov, Fiz. Tverd. Tela 12, 1189 (1970) [Sov. Phys. Solid State 12, 926 (1970)]; T. Skettrup and I. Balslev, Phys. Status Solidi 40, 93 (1970).

[5]J. E. Rowe, F. H. Pollak, and M. Cardona, Phys. Rev. Letters 22, 933 (1969).

[6]T. Koda, T. Mitani, and T. Murahashi, Phys. Rev. Letters 25, 1495 (1970).

[7]S. Sakoda and Y. Onodera, J. Phys. Chem. Solids 32, 1365 (1971).

[8]K. S. Song, J. Phys. Chem. Solids 28, 2003 (1967); J. Phys. (Paris) 28, 195 (1967).

[9]K. Shindo, A. Morita, and H. Kamimura, J. Phys. Soc. Japan 20, 2054 (1965).

[10]M. Cardona, Phys. Rev. 129, 69 (1963).

[11]W. Staude, Phys. Status Solidi 43, 367 (1971).

[12]G. Dresselhaus, Phys. Rev. 100, 580 (1955).

[13]G. L. Bir and G. E. Pikus, Fiz. Tverd. Tela 3, 3050 (1961) [Sov. Phys. Solid State 3, 221 (1962)].

[14]T. Inoguchi, T. Okamoto, and M. Koba, Sharp Tech. J. 12, 59 (1969).

[15]V. M. Agranovich and V. L. Ginzburg, *Spatial Dispersion in Crystal Optics and the Theory of Excitons* (Interscience, New York, 1966).

[16]In our present exciton problem, the second-order term of Eq. (8) has two sources. One is the kinetic energy associated with the translational motion of exciton. We can neglect this because of the heavy exciton mass in CuCl. The other is due to the stress-induced k-linear terms. They add higher-order terms as well as a linear one to the dielectric tensor. It is those higher-order terms that gives rise to the clamping effect mentioned in Sec. III C. We can neglect them again however so long as we are concerned with small stress. We thus neglect them and retain only the term linear in K.

[17]J. E. Nye, *Physical Properties of Crystals* (Oxford U. P., Oxford, England, 1957); L. D. Landau and E. M. Lifshitz, *Electrodynamics of Continuous Media*, translated by J. B. Sykes and J. S. Bell (Pergamon, New York, 1960).

[18]J. J. Hopfield and D. G. Thomas, J. Phys. Chem. Solids 12, 276 (1960).

[19]J. J. Hopfield, J. Appl. Phys. 32, 2277 (1961).

[20]G. D. Mahan and J. J. Hopfield, Phys. Rev. 135, A428 (1964).